

# Physics Plan at JLC

**Toshiaki Tauchi**

*KEK, High Energy Accelerator Research Organization, 1-1 Oho,  
Tsukuba-shi, Ibaraki-ken, 305-0810, Japan. E-mail address: toshiaki.tauchi@kek.jp*

We briefly report on the physics plan at JLC  $e^+e^-$  linear collider. The present status of JLC project is also described including R&D status of the major accelerator components.

## 1 Introduction

The  $e^+e^-$  Linear Collider project, so called JLC, is the next principal project for research in high energy physics in Japan[1]. The JLC project consists of two experimental phases. The first phase (JLC-1) is an  $e^+e^-$  linear collider at  $250 < \sqrt{s} < 500\text{GeV}$ [2], and the second phase will extend the center-of-mass energy to  $> 1\text{TeV}$ [1, 3]. Although the JLC was originally proposed as a national project more than 10 years ago, the recent Subcommittee on Future Projects of High Energy Physics in Japan recommended that "the Linear Collider should be hosted by Japan, and while the construction will be realized by international collaboration with Japan playing a key role, the experiment will be done on an international and open collaboration basis"[1].

In this spring, Asian Committee for Future Accelerators (ACFA) has initiated a physics and detector working group[4] under ACFA, considering the importance of the linear collider project and the potential of our community to realize it. The charge of the group is "to elucidate physics scenario and experimental feasibilities and to write up a report to ACFA within two years".

## 2 Physics Target and Scenario

In spite of the great success, the standard model can not be the final theory of elementary particles, since it has many arbitrary parameters such as masses of quarks/leptons and three gauge-coupling constants without unification. Regarding the incompleteness, future colliders must probe physics beyond the standard model. There are two physics scenarios beyond the standard model, which are technicolor[5] and supersymmetry[6] models.

In the technicolor model, a Higgs boson is taken over by three Goldstone bosons which appear when a chiral symmetry of techni-quarks is broken by their condensation. Although the idea of the dynamical symmetry breaking is very fascinating[7], the QCD-like technicolor model is definitely inconsistent with precise measurements of electroweak parameters at LEP-1[8]. Walking technicolor was not ruled out by them[9], however the phenomenology is very difficult because of its non-perturbative nature.

There is no satisfactory model based on the technicolor to explain a large mass of top quark.

In contrast, the supersymmetry has elementary Higgs bosons without a naturalness problem. Since the supersymmetry cancels the quadratic divergence of the Higgs mass due to radiative correction by pairs of particle- and sparticle-loops, the Higgs mass remains at the electroweak scale ( $v=246\text{GeV}$ ) even when there is a large energy scale such as a grand unification scale ( $M_{GUT} = 10^{16}\text{GeV}$ ) or the Planck scale ( $M_P = 10^{19}\text{GeV}$ ). Recent precise measurements show that three couplings of the standard model ( $SU(2)_L \times U(1)_Y \times SU(3)_C$ ) can not converge into a single value without the supersymmetry[10]. In addition, the heavy top quark can provide a radiative symmetry breaking with its large Yukawa coupling for the Higgs mechanism[11]. Thus, the supersymmetric theory is the most probable as physics beyond the standard model. Because of the perturbative theory, it has detailed physics predictions confronting experiments as described in following sections.

As mentioned above, the Higgs mechanism has never been experimentally verified in the standard model. So the discovery and detailed study of the Higgs boson is the most urgent experimental task for high energy physics. The upper limit of the Higgs boson mass has been reported to be  $280\text{GeV}$  at 95% confidence limit by a global electroweak fit based on all experimental data in the framework of the standard model[12]. The lightness of the Higgs boson mass is a good news for the supersymmetry. Actually, the upper bound is  $130\text{GeV}$  in the minimal supersymmetric standard model (MSSM). Generalized supersymmetric model predicts for the upper bounds of the lightest Higgs boson mass to be  $150\text{GeV}$  and  $180\text{GeV}$  with a gauge singlet and extra matter multiplets, respectively[13]. So the energy range of the JLC-1 is right for the Higgs study.

At JLC-1, discovery of the light Higgs boson must be dawn to the supersymmetric world. By precise measurements of branching ratios of the Higgs boson decaying to  $b\bar{b}$ ,  $c\bar{c}$ ,  $gg$  and  $\gamma\gamma$ , the supersymmetric Higgs boson can be discriminated from the standard model Higgs boson. If additional Higgs bosons such as H(heavy), A(pseudo-scalar) and  $H^\pm$ (charged) are found, the supersymmetry is verified experimentally with no doubt. The next step is the discovery and precise measurement of supersymmetric particles in order to determine supersymmetric parameters of  $m_0$ (common scalar mass),  $\mu$ (higgsino mass),  $M_2$ (gaugino mass) and  $\tan\beta \equiv v_2/v_1$ (ratio of vacuum expectation values) for the case of the minimal supergravity (SUGRA) model[14]. If successful, we could see through physics at the grand unified world and even at the Planck world since the supersymmetric scenario has a grand desert between the electroweak and grand unified worlds.

### 3 Overview of Physics and Detector

Figure 1 shows cross sections of the standard models, which are muon pair ( $\mu^+\mu^-$ ), five flavored quark pair ( $\Sigma q\bar{q}$ ), top quark pair ( $t\bar{t}, m_t=175\text{GeV}$ ), gauge boson pairs ( $ZZ$  and  $W^+W^-$  in  $|\cos\theta| < 0.8$ ) and Higgs boson ( $Zh, m_h=120\text{GeV}$ ) productions, and sparticles of the minimal supersymmetric model, which are scalar muon pair ( $\tilde{\mu}_{R(L)}^+\tilde{\mu}_{R(L)}^-$ )

,  $m_{\tilde{\mu}_{R(L)}^\pm} = 140(230)\text{GeV}$ , chargino pair ( $\tilde{\chi}^+\tilde{\chi}^-$ ,  $m_{\tilde{\chi}^\pm} = 220\text{GeV}$ ) and additional Higgs boson pairs ( $H^+H^-$ ,  $m_H = 190$  and  $410\text{GeV}$ ,  $HA$ ,  $m_H = m_A = 400\text{GeV}$ ). The event rates are also indicated by the right axis in Fig.1 for the integrated luminosity of  $50\text{fb}^{-1}$ . Since the design luminosities of the JLC are  $4.13, 8.28$  and  $16.72 \times 10^{33}\text{cm}^{-2}\text{sec}^{-1}$  at  $\sqrt{s} = 250, 500$  and  $1000\text{GeV}$ , respectively[3], many interesting processes of more than 5,000 events can be produced annually. Especially, the large statistics of  $W$  boson

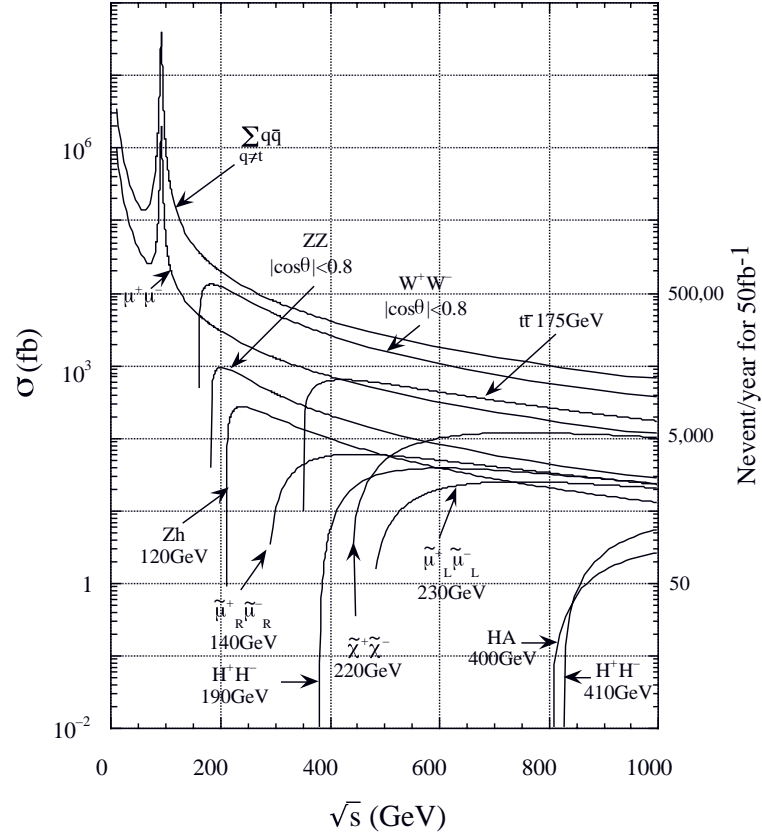


Fig. 1: Various cross sections( $\sigma(\text{fb})$ ) of  $e^+e^-$  collisions at  $\sqrt{s} < 1\text{TeV}$ . The left axis scales cross sections in fb, and the right axis shows yields for the integrated luminosity of  $50\text{fb}^{-1}$  which is the annual luminosity with a typical luminosity of  $5 \times 10^{33}\text{cm}^2\text{sec}^{-1}$ .

pairs allows us to probe the anomalous couplings of  $\delta\kappa_{Z,\gamma}, \lambda_{Z,\gamma}$  with a high precision of  $O(1\%)$  at  $\sqrt{s} = 500\text{GeV}$ [2]. Top quark pairs are also created in similar amount to  $\mu$  pairs. Assuming the QCD corrections are precisely known, top quark mass can be determined with  $\delta m_t/m_t = 0.1\%$  only for  $10\text{fb}^{-1}$ , and the total decay width can be mea-

sured with 5% accuracy for  $100 \text{ fb}^{-1}$ . The Yukawa coupling to Higgs boson can be also obtained with 25% accuracy by the energy scan over toponium states for  $10 \text{ fb}^{-1}$ [2]. In the subsequent sections, physics of Higgs boson and supersymmetric particles are discussed in some details.

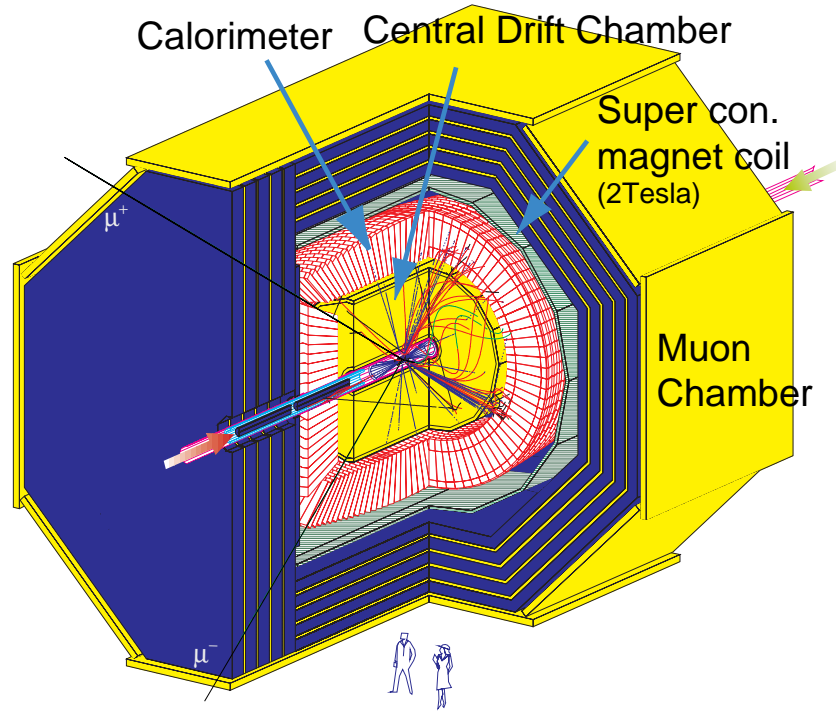


Fig. 2: Schematic view of the JLC detector. The total volume is  $16 \times 16 \times 16 \text{ m}^3$ , and it weighs 15,000 tons. A simulated event of Higgs boson production ( $e^+e^- \rightarrow Zh, h \rightarrow b\bar{b}, Z \rightarrow \mu^+\mu^-$ ) is also superimposed for  $m_h=120\text{GeV}$  at  $\sqrt{s}=300\text{GeV}$ , where the simulation is based on GEANT3.21[15].

In  $e^+e^-$  annihilation into hadrons ( $e^+e^- \rightarrow q\bar{q}$ ) at  $\sqrt{s}=500\text{GeV}$ , about 80 particles are created on average, where a half of them is neutral particles. They are clustered into jets which become narrower at higher center-of-mass energy of  $e^+e^-$  collisions. One of goals of JLC detector is to identify the jets as quarks and gluons. Since a large fraction of gauge bosons ( $W, Z$ ) decays into two quarks (jets), good energy and momentum resolutions are required for the measurements of charged and neutral particles inside the jets. The resolution of invariant mass of the two jets should be comparable with the natural widths of gauge bosons ( $\Gamma_W=1.8\text{GeV}, \Gamma_Z=2.5\text{GeV}$ ). For the performance

specification of tracking detector, a process of Higgs boson production ( $e^+e^- \rightarrow Zh$ , then  $Z \rightarrow \ell^+\ell^-$ ) has been chosen. In this process, the mass of Higgs boson can be obtained by the recoil mass method, that is  $m_h^2 = (\sqrt{s} - (E_{\ell^+} + E_{\ell^-}))^2 - (p_{\ell^+} + p_{\ell^-})^2$ . Therefore a good momentum measurement of two leptons( $\ell^\pm$ ) is required so that it gets close to the beam-energy resolution of 0.13% to be realized under the optimal condition. In addition, it is essential to have good tagging efficiencies of bottom (charm) quarks in jets for the identifications of Higgs ( $h \rightarrow b\bar{b}$ ) and top ( $t \rightarrow bW$ ).

Under these considerations, JLC group proposed a general purpose detector[2] as shown in Fig.2. All the major apparatuses are located inside of 2-tesla superconducting magnet in order to minimize materials between the central drift chamber and calorimeter. The angular coverage is  $|\cos\theta| < 0.98$ . The energy resolutions of the calorimeter are  $\sigma_E/\sqrt{E} = 15\%/\sqrt{E} \oplus 1\%$  and  $\sigma_E/\sqrt{E} = 40\%/\sqrt{E} \oplus 2\%$  for electrons/photons and hadrons, respectively. The momentum resolution of the central drift chamber is  $\sigma_{p_t}/p_t = 1.1 \times 10^{-4} p_t \oplus 0.1\%$ . At the center of the detector very close to the interaction point, there is a vertex(CCD) detector, whose innermost radius is 2.5cm from the beam line, to tag bottom quarks. The impact parameter resolution is  $\delta^2 = 11.4^2 + (28.8/p)^2/\sin^3\theta(\mu\text{m}^2)$ .

The performances mentioned above are assumed in following physics simulations together with the general properties of  $e^+e^-$  collisions such as the initial state radiation and beamstrahlung[16] at JLC.

## 4 Physics Topics

### 4.1 Higgs

The major process of Higgs boson production is  $e^+e^- \rightarrow hZ$  at  $\sqrt{s} < 500\text{GeV}$ . Because of the "cleanness" of  $e^+e^-$  collisions, the discovery of Higgs boson is relatively easy. Possible backgrounds are  $e^+e^- \rightarrow ZZ$ ,  $e^+e^- \rightarrow W^+W^-$  and  $e^+e^- \rightarrow e\nu W$ . The last two processes can be easily reduced by good b-tagging since they do not decay to bottom quarks while Higgs boson dominantly decays into  $b\bar{b}$ . In general, it is very important to have a good invariant mass resolution of two jets especially for the case of  $m_h$  close to  $m_Z$ . The most model-independent way to discover the Higgs boson is the recoil mass method ( $e^+e^- \rightarrow hZ$ ,  $Z \rightarrow \ell^+\ell^-$ ) as mentioned in the previous section, which is independent of Higgs decay modes, so the Higgs boson decaying into invisible particles (SUSY-LSP etc.) can be also discovered. Figure 3 shows the recoil mass distributions for  $m_h=80, 100, 120$  and  $140\text{GeV}$  at  $\sqrt{s}=300\text{GeV}$  for the integrated luminosity of  $30\text{fb}^{-1}$ . They are simulated for two cases of beam energy spread, which are 2%(nominal) and 0.13%(precision) full width in the upper(a) and lower(b) figures, respectively. For both cases, the Higgs boson can not escape detection, although the precision mode of machine operation enhances the Higgs boson peak and it will reveal its real power for  $m_h$  overlapping  $m_Z$ [2].

If only one Higgs boson is found without new particles, the precision measurements of cross sections and decay branching ratios are very important to search for physics beyond the standard model. In the minimal supersymmetric model(MSSM), the Higgs

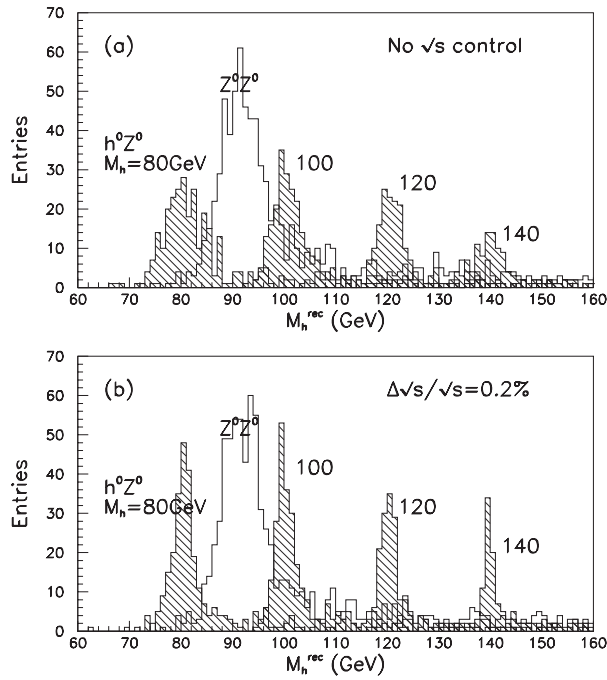


Fig. 3: Recoil mass distributions for various Higgs boson masses ( $m_h=80, 100, 120$  and  $140\text{GeV}$ ) in  $e^+e^- \rightarrow hZ, Z \rightarrow \ell^+\ell^-$  together with the background process of  $e^+e^- \rightarrow ZZ$  at  $\sqrt{s}=300\text{GeV}$  for the integrated luminosity of  $30\text{fb}^{-1}$ , under (a) the nominal machine condition and (b) the precision one of "minimal beam energy spread" ( $\delta\sqrt{s}/\sqrt{s}=0.2\%$ ). The recoil mass was reconstructed by two momenta of leptons and the well-known beam energy, where the momenta were smeared with the resolution specified in the text.

sector can be described by two parameters ( $m_A, \tan\beta$ ). Since the major decay mode of  $h \rightarrow b\bar{b}$  is also a function of these parameters in the MSSM, the cross section times the branching ratio ( $\sigma(Zh) \times Br(h \rightarrow b\bar{b})$ ) significantly differs from the standard model as shown in Fig.4. Generally at large  $m_A$ , when  $\tan\beta$  becomes larger,  $Br(h \rightarrow b\bar{b})$  is getting larger too, then deviating from that of the standard model. Our detailed Monte Carlo simulation shows that about 2,000 Higgs bosons can be observed in the final states of  $\nu\bar{\nu}b\bar{b}$  and  $q\bar{q}b\bar{b}$  for the integrated luminosity of  $80\text{fb}^{-1}$ . Therefore,  $\sigma(Zh) \times Br(h \rightarrow b\bar{b})$  will be measured with 2% accuracy ( $1\sigma$ ). As seen in Fig.4, this measurement can probe the validity of the standard model in the large region of interesting parameter space. The precision measurements of other decay modes are also useful to determine the MSSM parameters[18].

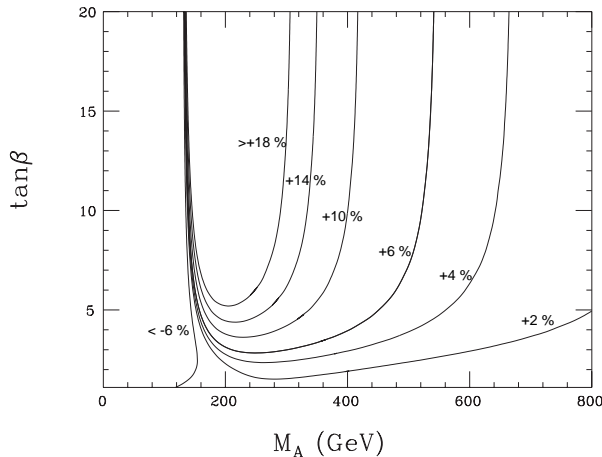


Fig. 4: Contours of deviation of  $\sigma(Zh) \times Br(h \rightarrow b\bar{b})$  from the standard model in a plane of  $\tan\beta$  and  $m_A$  (MSSM), where  $m_t=175\text{GeV}$ [17]. The region of  $m_A < 250\text{GeV}$  can be probed by direct observation of  $A$  and  $H$  in  $e^+e^- \rightarrow ZH, HA$  at  $\sqrt{s}=500\text{GeV}$ .

## 4.2 SUSY (Scalar Tau Production)

There is no problem to observe supersymmetric particles if the center-of-mass energy exceeds the threshold of the pair creation. Since the electron beam can be polarized with more than 90%, the  $e^+e^-$  linear collider should be the best in order to investigate the supersymmetric model.

The most interesting example is a pair production of scalar tau (stau or  $\tilde{\tau}$ )[19, 20]. Scalar tau may be the lightest scalar leptons because of large mixing between  $\tilde{\tau}_L$  and  $\tilde{\tau}_R$  due to the non-negligible Yukawa coupling. With the mixing angle of  $\theta_\tau$ , a lighter stau ( $\tilde{\tau}_1$ ) can be expressed by  $\tilde{\tau}_1 = \tilde{\tau}_L \cos\theta_\tau + \tilde{\tau}_R \sin\theta_\tau$ .  $\tilde{\tau}_1$  is assumed to decay into  $\tilde{\chi}_1^0\tau$ , where  $\tilde{\chi}_1^0$  is the lightest neutralino. The detailed simulation shows that the masses of  $\tilde{\tau}_1$  and  $\tilde{\chi}_1^0$  can be determined from the measurement of energy distribution of  $\rho$  ( $\tau \rightarrow \rho\nu$ ) with 1% accuracy at  $\sqrt{s}=500\text{GeV}$  for the integrated luminosity of  $100\text{fb}^{-1}$ , where masses of  $\tilde{\tau}_1$  and  $\tilde{\chi}_1^0$  are assumed to be 150 and 100 GeV, respectively[20]. The mixing angle can be determined by the measurement of cross section with a right-handed polarized electron beam of  $P_e=95\%$ , since the exchanged gauge boson is almost Bino( $\tilde{B}$ ) which couples to the hypercharge( $Y$ ) of  $\tilde{\tau}_1$  consisting of  $\tilde{\tau}_L(Y=-1/2)$  and  $\tilde{\tau}_R(Y=-1)$ . The simulated result was  $\delta \sin\theta_\tau=0.049$  correlating with  $m_{\tilde{\tau}_1}$  largely.

Tau polarization also has a very important information on  $\tan\beta$ [19]. The reason is as follows. In general, the neutralino ( $\tilde{\chi}_1^0$ ) is a mixing state of gaugino and higgsino. The gaugino coupling preserves a helicity of stau while the higgsino coupling flips it in  $\tilde{\tau}_1 \rightarrow \tau\tilde{\chi}_1^0$ . Actually the helicity-flip is caused by the Yukawa interaction which is proportional to  $m_\tau/\cos\beta$ . Therefore, the measurement of  $\tau$  polarization should be

sensitive to  $\tan\beta$ .

Since  $\sin\theta_\tau$ ,  $\tan\beta$ ,  $m_{\tilde{\tau}_1}$  and  $m_{\tilde{\chi}_1^0}$  are all correlated, their measurement errors can be significantly reduced if one of them can be measured precisely. The example is the measurement of scalar electron ( $\tilde{e}_R$ ) pair production to determine  $m_{\tilde{\chi}_1^0}$ . Form such an analysis,  $\tan\beta$  can be measured well for the higgsino-like region of  $\tilde{\chi}_1^0$  ( $M_1 > 150$  GeV, where  $M_1$  is a gaugino mass of U(1)-symmetry)[20].

## 5 R&D status of the Accelerator

The JLC consists of three major systems of pre-acceleration, main acceleration and final focus as shown in Fig.5[3]. The pre-acceleration system produces a high quality

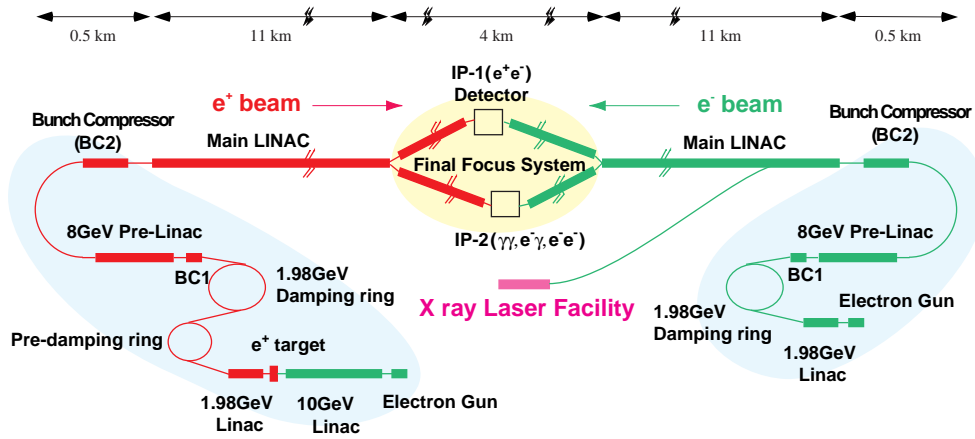


Fig. 5: Schematics of JLC accelerator complex ( $0.25\text{TeV} < \sqrt{s_{e^+e^-}} < 1.0\text{TeV}$ ).

beam to be injected into the main linear accelerator(linac). First, a high intensity beam( $7.0 \times 10^9$ /bunch) is created with a multi-bunch structure (85 bunches/RF pulse) by a thermionic-electron gun at 150Hz. In a 1.98GeV damping ring, the emittance of the beam is reduced so that the divergence times the cross section of the beam shrinks by about 1/100 of what has been achieved so far. At the positron beam line, there are an additional 10 GeV electron-linac to create positrons at  $e^+$  target and a pre-damping ring with a large positron capture efficiency. The bunch length of the beam is compressed from  $\sim 5\text{mm}$  to  $\sim 0.1\text{mm}$  by bunch compressors in order to be efficiently accelerated at the main linac. In the main acceleration system (main linac), the beam is accelerated with the average gradient of 55.6MeV/m by a 11.4GHz(x-band) RF system consisting of klystrons and accelerating cavities. Collimating the beam to control beam-related backgrounds at the interaction point, the beam is strongly focussed to  $3\text{nm}(\sigma_y)$  and  $260\text{nm}(\sigma_x)$  in vertical and horizontal directions, respectively, in the final focus



system. The design luminosity is  $8.28 \times 10^{33} \text{cm}^{-2} \text{sec}^{-1}$  at  $\sqrt{s}=500 \text{GeV}$ . There are two interaction points with their own final focus systems. The motivation of the second interaction point is for  $\gamma\gamma$ ,  $e^- \gamma$ , and  $e^- e^-$  collisions for complementary physics to  $e^+ e^-$ [21]. Also, JLC may have an X ray laser facility for material physics[2].



Fig. 6: ATF Linac viewed from the upstream.

As one of key elements to produce an ultimately low emittance beam for JLC, the Accelerator Test Facility (ATF) has been constructed at KEK in Japan. The ATF consists of a 1.54GeV damping ring and a injection-linac together with an extraction line to measure the beam profile, that is the emittance. The ATF-linac, which is 70 m long with 9 s-band (2,856MHz) klystrons of 85MW power, has been operating at the average accelerating gradient of 30MeV/m since autumn 1995. The ATF-damping ring is a race-track shaped accumulation ring of  $\sim 120 \text{m}$  circumference. At the two straight sections, multiple wiggler magnets are located to increase the radiation damping effect necessary at 150Hz operation. The injected beam of 1mm diameter must be squeezed down to  $40 \mu\text{m}$  (horizontal)  $\times$   $6 \mu\text{m}$  (vertical) at the exit within the damping time. Since the commission in January 1997, its performance has been investigated in great detail including a seasonal ground movement of the floor. At present, the design value of the (unnormalized) horizontal emittance was achieved to be 1nm, while the vertical one is still larger by about 5 times, where the coupling (the vertical/horizontal ratio) should be 1% in the design. Upgrading the beam position monitors in the ring as well

as re-alignment of magnets and the bunching section in the linac during this summer shutdown, it is expected to achieve the design vertical emittance by the end of this year[22].



Fig. 7: ATF Damping Ring.

RF power sources are the x-band klystrons in the main linac. The R&D goals of the x-band klystrons are the peak output power of 75MW and the RF efficiency of 47% operating with  $1.5\mu\text{sec}$  pulse width at the repetition rate of 150pps. The last solenoid-focused klystron of XB72K-no.9 produced a output power of 72MW with 200nsec pulse width and 31% efficiency. The power is not limited by itself but by a high voltage modulator at present. A successful 3 dimensional simulation (MAGIC) shows that it can attain 75 MW with  $1.5\mu\text{m}$  pulse width. Also, BINP(Russia) group designed and fabricated a PPM (Periodic Permanent Magnet) focused klystron in a collaboration with KEK. The PPM klystron has been tested at KEK. The output power was 77.4 (55)MW with 100 (430)nsec pulse width and 38 (33)% efficiency, which were limited by RF instabilities. The instabilities were also estimated by simulation with MAGIC to be caused by particle interception in the output structure. All the klystrons which have been made so far were designed by a one-dimensional simulation program (DISKLY). As briefly mentioned above, KEK successfully developed the three dimensional simulation program based on MAGIC, which explains all the performances of previous klystrons very well. We are waiting for XB72K-no.10 which was first designed by the MAGIC. The XB72K-no.10 is under construction and is expected to produce a peak output power of 126MW with  $1.5\mu\text{sec}$  pulse width and 48.5% efficiency. It will be tested in this November[23].

As a backup of the x-band main linac system, a c-band RF system has been also developed[24], where the c-band (5,712MHz) is half a frequency of the x-band. Especially, the c-band klystron has been tested in August 1997. The peak output power was 50 (46.4)MW with 1 (2.5) $\mu$ sec and 43 (42)% efficiency operating at 20 (50) pps. Such performance already satisfies the requirement of JLC-1. Since then, the klystron has been continuously operated for the lifetime test at 50 or 25 pps for 4 months without any problem on the klystron itself.

There are many other R&D programs at KEK in collaboration with many universities and countries. Getting very encouraging results of the R&D, we are confident about technology to realize JLC in very near future.

## 6 Conclusion

The center-of-mass energy region of  $250 < \sqrt{s} < 500$ GeV has been shown to be very important to know the physics beyond the standard model. The supersymmetric model can be definitely proved or disproved by discovery of the light Higgs boson. Thus the experimental study in this energy region will lead us to a definite choice of a new physics scenario beyond the standard model.

The road map for JLC project was recently presented by KEK Director General at the XXIX International Conference on High Energy Physics (ICHEP98) held in Vancouver. In short, aiming to start its construction in Japan in Fiscal Year 2003, the Japanese HEP community will decide early in 2000 whether to go for the design of their own or common to SLAC. Possible regional framework of cooperation will be discussed first in ACFA around that time, and its further extension probably in 2001 when reformed government ministries are expected to start. Although the LHC experiments will have started when JLC is commissioned, there is no doubt that  $e^+e^-$  physics will be essential to discovery of light Higgs boson as well as detailed and high-precision studies on the Higgs, top quark, supersymmetric particles and gauge bosons.

## 7 Acknowledgement

The author would like to thank all the members of JLC physics and accelerator groups for useful discussions on recent progress of the JLC project. He also thanks Professor S. Iwata, the head of JLC Promotion office at KEK, for valuable comments on the manuscript.

### References

- [1] *The Final Report of the Subcommittee on Future Projects of High Energy Physics in Japan*, High Energy News Vol.17, May 1998. The report can be also obtained from a ftp-site of <ftp://ftp/kek.jp/kek/HEPSC/final/>.
- [2] JLC Group: *JLC-1 (Green Book)*, KEK Report 92-16, December 1992, see also <http://www-jlc.kek.jp/JLC.proposal-j.html>.

- [3] JLC Design Study Group: *JLC Design Study*, KEK Report 97-1, April 1997, see also <ftp://lcdev.kek.jp/pub/DesignStudy/>.
- [4] ACFA Joint Linear Collider Physics and Detector Working group: the detailed informations can be obtained from the home page of <http://acfahep.kek.jp/>.
- [5] E. Farhi and L. Susskind: *Phys. Rep.* **74** (1981) 277; , and references therein.
- [6] D.V. Volkov and V.P. Akulov: *Phys. Lett.* **46B** (1973) 109; , J. Wess and B. Zumino: *Nucl. Phys.* **B70** (1974) 39; .
- [7] K. Lane: *Talk given at International Conference on the History of Original Ideas and Basic Discoveries in Particle Physics, Erice, Italy, 29 Jul - 4 Aug 1994*, BUHEP-94-26, Oct 1994. e-Print Archive: hep-ph/9501249
- [8] B. Jacobsen: *QCD and High Energy Hadronic Interactions (Proceedings of the XXIXth RECONTRÉ DE MORIOND)*, p531-538, Editions Frontieres, 1994.
- [9] K. Lane: *HIGH ENERGY PHYSICS (proceedings of 27th International Conference on High Energy Physics (ICHEP), Glasgow, Scotland, 20-27 Jul 1994)* edited by P.J. Bussey and I.G. Knowles, IOP, pp.543-548,1995.
- [10] P. Langacker and N. Polonsky: *Phys. Rev.* **D47** (1993) 4028;
- [11] K. Inoue, A.Kakuto, H. Komatsu and S. Takeshita: *Prog. Theor. Phys.* **68** (1982) 927; ,**71** (1984) 348, L.E. Ibáñez and G.G. Ross: *Phys. Lett.* **110B** (215) ; ; L. Alvarez-Gaumé, J. Polchinsky and M.B. Wise: *Nucl. Phys.* **B221** (1983) 495; , J. Ellis, J.S. Hagelin, D.V. Nanopoulos and K. Tamvakis: *Phys. Lett.* **125B** (1983) 275; .
- [12] D. Karlen: *Talk presented at the International Conference on High Energy Physics (ICHEP98)*, Vancouver, Canada, July, 1998.
- [13] T. Moroi and Y. Okada: *Phys. Lett.* **295B** (1992) 73; .
- [14] T. Tsukamoto et al.: *Phys. Rev.* **D51** (1995) 3153; .
- [15] GEANT3.21-Detector Description and Simulation Tool, Application Software Group, computing and networks division, CERN, CERN Program Library Long Writeup W5013, March 1994.
- [16] K. Yokoya and P. Chen: "Electron energy spectrum and maximum disruption angle under multi-photon beamstrahlung", presented at *the IEEE Particle Accelerator Conference, Chicago, 1989*, SLAC-PUB-4935(1989).
- [17] A. Miyamoto, private communication.
- [18] M.D. Hildrech, T.L. Barklow and D.L. Burke: *Phys. Rev.* **D49** (1994) 3441; , K. Kawagoe and I. Nakamura: *Phys. Rev.* **D54** (1996) 3634; , J. Kamoshita: OCHA-PP-109, February 1998, hep-ph/9802203.
- [19] M.M. Nojiri: *Phys. Rev.* **D51** (1995) 6281; .
- [20] M.M. Nojiri, K. Fujii and T. Tsukamoto: *Phys. Rev.* **D54** (1996) 6756; .
- [21] I. Watanabe *et al.*:  *$\gamma\gamma$  Collider as an Option of JLC*, KEK Report 97-17, March 1998.
- [22] J. Urakawa *et al.*: "Recent Results on KEK/ATF Damping Ring", contributed paper to the XVIIth International Conference on High Energy Accelerators, September 7-12, 1998, Dubna, KEK Preprint 98-154, September 1998.
- [23] Y.H. Chin *et al.*: "The 120MW X-band Klystron Development at KEK" contributed paper to The Sixth European Particle Accelerator Conference (EPAC98) Stockholm, Sweden, Jun 22 - 26, 1998, KEK Preprint 98-118, August 1998.
- [24] T. Shintake *et al.*: "Results from Hardware R&D on C-band RF-system for  $e^+e^-$  Linear Collider", contribution paper to The XIX International Linear Accelerator Conference (LINAC98), Chicago, USA, August 23-28, 1998, KEK Preprint 98-139, October 1998.